Fingering Instability in Combustion

Ory Zik,[1] Zeev Olami,[2] and Elisha Moses[1]

[1]*Department of Physics of Complex Systems, The Weizmann Institute of Science, Rehovot 76100, Israel*
[2]*Department of Chemical Physics, The Weizmann Institute of Science, Rehovot 76100, Israel*

A thin solid, burning against an oxidizing wind, develops a fingering instability. The effect is observed in a narrow gap geometry, where free convection is suppressed. Focusing on the developed nonlinear state, we find that two length scales coexist. The spacing between fingers is determined by the Péclet number, and the finger width is determined by heat losses. Dense fingers develop by tip splitting. A phenomenological model accurately predicts the fingers' spacing, and is generally applicable to diffusion limited systems. We suggest that the effect is a new, accurately controllable, version of the thermal-diffusive instability. [S0031-9007(98)07473-0]

Combustion is a complex chemical reaction involving tens of concurrent processes [1,2]. It is further complicated by instabilities at the combustion front, which determine the flame dynamics and shape. The problem can be simplified by noticing that it is governed by the availability of its basic constituents: fuel, oxidant, and heat. This leads to a number of instabilities, of which the most pertinent comes from the competition between the destabilizing molecular transport and the stabilizing heat transfer—the thermal-diffusive instability in "premixed" flames [2,3].

In this paper we report a new effect: a combustion front in a quasi-two-dimensional geometry exhibits a *directional fingering instability* with two length scales that are determined differently (the finger width w and the spacing between fingers d). The nondimensional control parameter is the Péclet number Pe which measures the relative importance of molecular advection and diffusion. This fingering effect has been independently observed in a recent experiment conducted in space [4]. We show that the correspondence between the two experiments is due to the suppression of free convection. From the practical viewpoint, our results show that a slow persistent finger of fire can exist in an oxygen-rich thin gap well below the limits of conventional detection.

Previous studies of flame propagation over thin solid fuels have focused mainly on the rate of flame spread and on roughness [5]. A cellular structure observed in this system was recently related to the thermal-diffusive instability [6]. On the theoretical side, recent work predicts a connection between the Saffman Taylor instability and two-dimensional filtration combustion [7]. Stability of one-dimensional fronts has been extensively studied in simpler, less reactive, growth systems than combustion [8].

The experimental setup is shown schematically in Fig. 1. It is based on a horizontal, thin gap geometry, the incoming reactant gas flowing between two plates. The top plate is glass, allowing visualization from above. The part of the bottom plate which touches the sample can be changed to allow a study of the effect of ambient heat conductivity. The thin fuel sample is stretched out straight onto the bottom plate. The experiment is initiated by uniformly igniting the fuel along a line near its downstream edge (details will be given in [9]). The main experimental controls are the flow velocity of oxygen V_{O2} and the adjustable vertical gap between top and bottom plates h. The oxidizing gas is supplied in a uniform laminar flow (as verified and calibrated by flow visualization with smoke), opposite to the direction of the front propagation (i.e., the fuel and oxygen are fed to the reaction from the same side). This configuration enhances the destabilizing effect of reactant transport.

The measurements are performed in the slow combustion regime termed smoldering. This is a "nonflaming" mode of combustion (i.e., the emitted gas does not "glow" in the visible light) where oxygen interacts with a solid fuel to produce char, gaseous products, and the heat that sustains the process [7]. This regime is convenient to control experimentally. The "fuel" is typically filter paper (Whatman #2, 20×20 cm^2). However, the effect is fuel independent. In many materials the front involves melting and a glowing flame. Such complications in other fuels may change some quantitative aspects of instability, but
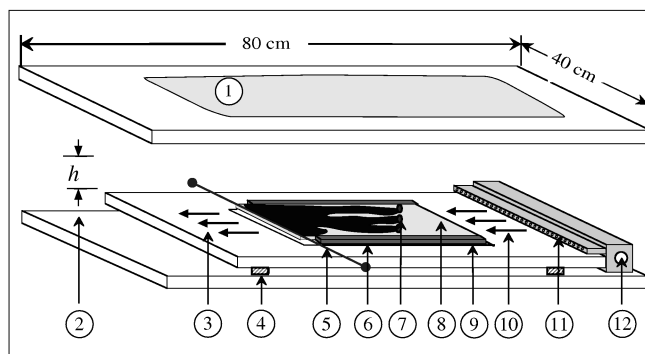

FIG. 1. Schematic representation of the setup. 1—glass top; 2—variable gap between top and bottom plates h; 3—outflow of combustion products; 4—spacers to control h; 5—ignition wire; 6—heat conducting boundaries; 7—flame front; 8—fuel; 9—interchangeable bottom plate; 10—uniform flow of O$_2$/N$_2$; 11—gas diffuser; and 12—gas inlet.

it is important to note that the fingering occurs in both the smoldering and the flaming regimes, and occurs in all the combustible materials that we examined (e.g., standard stationery paper, cellulose dialysis bags, and polyethylene sheets).

When V_{O2} is decreased below a critical value, the smooth front (Fig. 2a) develops a structure which marks the onset of instability (Fig. 2b). Further decreasing V_{O2} yields a cellular structure with a dominant wavelength (Fig. 2c). As V_{O2} is decreased further, the peaks are separated by cusplike minima, and a fingering pattern is formed. A typical fingering pattern is shown in Fig. 2d. The evolved state develops by recurrent tip splitting. Fingers that are closer to the oxygen source *screen* neighboring fingers from the source of oxygen. The screened fingers stop growing, and the tips of the screening fingers split. The splitting is such that both the average finger width and the spacing between the fingers remain unchanged. When V_{O2} is further decreased the spacing between fingers increases, and we obtain sparse fingers with no tip splitting (Fig. 2e). Combustion occurs only in the limited vicinity of the tip; there is no reaction behind the front (along the fingers).

Figures 2c–2e shows the existence of two well-defined length scales in the fingering pattern, the average finger width w, and the average spacing between fingers d. While w depends very weakly on V_{O2}, d is a rapidly decreasing function of it. The maximal value of d is comparable to the system size $d \sim L$. The minimal value of d (zero) is reached when the increase in oxygen flow wipes out the pattern (Fig. 2c). Tip splitting occurs for $d \sim w$.

While there is no theory as yet for the role of heat transport away from the front, a number of observations point to its crucial role. We shall show later that the heat transport determines the width of the finger w. Equally important, we find that the occurrence of the fingering instability coincides with the arrest of free convection of gas in the gap. The flame tip is a heat source with a temperature of approximately $T_f = 720$ K. Convection at the tip, while extremely inhomogeneous, is determined by the Rayleigh number Ra $= \frac{g\beta(T_f - T_{top})h^3}{\nu\alpha}$. $T_{top} \approx 450$ K is calculated by comparing the heat that is produced by the burning to the heat losses, the latent heat of evaporation, and the heat needed to bring the paper to its evaporation temperature [9]. $\nu = 0.5$ cm^2/s and $\alpha = 0.5$ cm^2/s are the kinematic viscosity and thermal diffusivity, respectively, at the estimated gas temperature $T_{gas} \approx 585$ K. $\beta \approx \frac{1}{T_{gas}}$ is the volumetric expansion coefficient. The onset of natural convection is expected at Ra$_c \approx 1700$ (neglecting the applied wind and nonuniform heating). Experimentally, fingering occurs for $h \leq 1$ cm, i.e., Ra ≥ 1810. The rough numerical agreement is an indication that fingering appears in the *absence of natural convection*. It also explains why the same phenomena has been observed in a microgravity experiment in space [4].

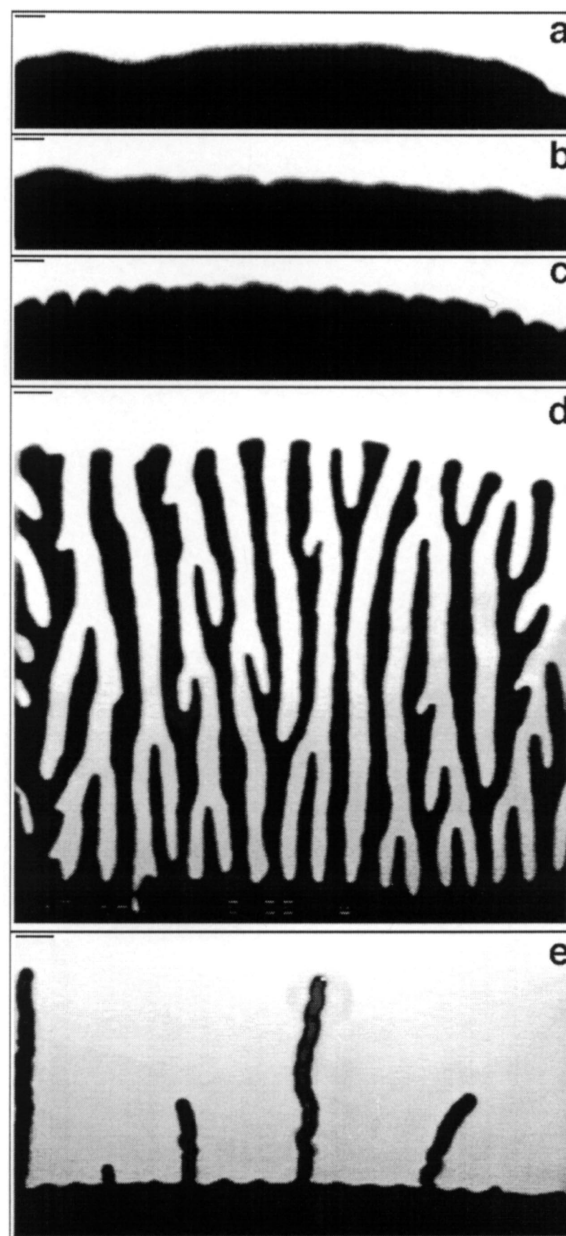In the absence of convection, transport of the incoming oxygen is dominated by diffusion and advection. The

FIG. 2. The instability as a function of oxygen flow V_{O2} [decreasing from (a) to (e)]. (a) smooth front; (b) irregular front; (c) periodic pattern; (d) fingering pattern with tip splitting; (e) fingering without tip splitting. The pattern defines two lengths: the finger width w and spacing between fingers d. Both lengths stabilize within a short initial transient. The scale bars are 1 cm. The gap between plates is $h = 0.5$ cm. The oxygen flow velocity V_{O2} is directed downwards, and the front velocity u is directed upwards. The values are (top to bottom) $V_{O2} = 11.4, 10.2, 9.2, 1.3, 0.1$ cm/s and $u = 0.5, 0.48, 0.41, 0.14, 0.035, \pm 0.01$ cm/s.

relation between the two is determined by the Péclet number, which in our quasi-2D configuration is Pe $= \frac{V_{O2}h}{D}$. We present a phenomenological model involving only these two mechanisms, which suffices to explain the details of the fingering instability. Dimensional analysis leads us to expect that the measured quantities u, d, and w

depend on the dimensional parameters h, V_{O2}, and D and on Pe. Thus, we nondimensionalize $\tilde{w} = \frac{w}{h}$, $\tilde{d} = \frac{d}{h}$, and $\tilde{u} = \frac{u}{V_{O2}}$.

A critical value Pe_c exists, below which the front is unstable, while above it a flat (though noisy) front propagates (Fig. 2). As the oxygen supply is decreased, small bumps that exist along the interface begin to compete for the oxygen. This mechanism resembles the thermal diffusive instability [2]. The consumption of oxygen drives lateral diffusion currents. When the oxygen supply is further decreased, the bumps consume all the oxygen that is available in their vicinity, and separate into distinct fingers. The "upstream" fingers (which are closer to the oxygen source) prevail and then tip split to maintain the same average d. As the oxygen supply is further decreased d increases. At a certain stage d is sufficiently large to allow fingering without screening (and tip splitting). Unlike d, w is independent of oxygen supply, but depends on heat losses from the front which are neglected in this simplified picture.

For Pe smaller than another critical value Pe_{c1} we observe well separated fingers. We regard the narrow band $Pe_{c1} \leq Pe \leq Pe_c$ as the onset regime for the instability. In this regime we observe a connected front with a cellular structure of typical size w. We expect Pe_c, as well as the characteristic length w, to be explicitly given by a linear stability analysis of the onset regime, which must include the effects of the heat transport.

Mass conservation.—In the oxygen limited case we expect all the available oxygen to be consumed and first write a mass conservation equation:

$$\tilde{u}\,\frac{\tilde{w}}{\tilde{w} + \tilde{d}} = A, \tag{1}$$

where $\frac{w}{w+d}$ is the fraction of burned area, integrated over the width of the sample L, and A is the stoichiometric factor $A = \frac{a\rho_{O2}(h-\tau_{ub})}{\mu(\rho_{ub}\tau_{ub} - \rho_b\tau_b)}$. Here μ is the stoichiometric coefficient, defined as the mass of reactant gas consumed by reacting with one unit mass of solid. ρ_{O2} is the oxygen density, a is the fraction of oxygen in the gas mixture, and τ is the fuel thickness. The subscripts b and ub stand for burned and unburned solids, respectively.

Equation (1) predicts a linear dependence (in dimensional units) of the quantity of burned material per unit time $uw/(w + d)$ on the input reactant velocity V_{O2}, and holds for $Pe \leq Pe_c$. This dependence is shown in Fig. 3. The measured slope is $A = 0.043 \pm 0.005$, compared with a predicted slope of $A = 0.051 \pm 0.005$ [10]. The numerical agreement (within experimental error) shows that the system is well within the oxygen deficient regime. Similar agreement is obtained for values of $a < 1$. The assumption that the depletion of oxygen is complete has been verified independently by measuring directly the percentage of oxygen in the output gas, using a commercial oxygen concentration detector (Emproco 020697, response 5 s, probe diameter 3 mm) inserted just behind the front [9].
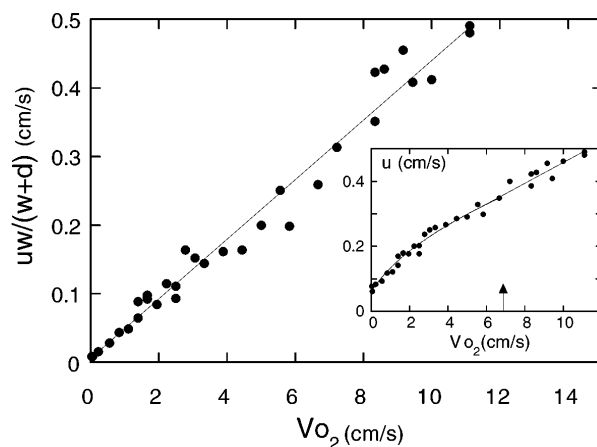
FIG. 3. Mass conservation, as predicted by Eq. (1). The inset shows u as a function of V_{O2}. The arrow corresponds to Pe_{c1}. We verified that Eq. (1) is also satisfied when the parameter being varied is the fraction of oxygen in the feeding gas ($0.5 \leq a \leq 1$), as well as for the case when the front propagates with the wind. The oxygen molecular diffusion coefficient is taken to be $D = 0.25$ cm^2/s, neglecting its temperature dependence.

Lateral diffusion.—The deficiency of oxygen produces concentration gradients and consequently lateral diffusion currents, which should be taken alongside with Eq. (1). These are given by $j_x = D\nabla_x C_{O2}$, where C_{O2} is the oxygen concentration. The gradient is approximated by the typical distance of $d + w$. To maintain steady state, the lateral current must satisfy $j_x = uC_{O2}$ up to a proportionality constant of order unity. This means that the propagation corresponds directly to the supply of oxygen by lateral (diffusion driven) currents. Combining these two relations for j we obtain

$$\tilde{u} = \frac{1}{(\tilde{w} + \tilde{d})}\,Pe^{-1}. \tag{2}$$

Combining Eqs. (1) and (2), we see that for $Pe \leq Pe_{c1}$ the finger width $\tilde{d}$ and velocity $\tilde{u}$ are given by

$$\tilde{d} = \sqrt{\frac{\tilde{w}}{A}}\,Pe^{-1/2} - \tilde{w}, \tag{3}$$

$$\tilde{u} = \sqrt{\frac{A}{\tilde{w}}}\,Pe^{-1/2}. \tag{4}$$

The measured front velocity u is shown in the inset of Fig. 3. Below Pe_{c1} (arrow in the figure), it behaves like $u \sim V_{O2}^{1/2}$, predicted by Eq. (4). At Pe_{c1} there is a crossover to the linear dependence predicted by Eq. (1) with $d = 0$.

Equation (3) also yields the critical Pe_{c1} for the onset of a connected front, where d goes to zero but the front is still unstable: $Pe_{c1} = \frac{1}{A\tilde{w}}$. Experimentally, $Pe_{c1} = 17 \pm 1$, while the predicted value is $Pe_{c1} = 1/Aw \approx 21$. For values of Pe in the onset range $Pe_{c1} \leq Pe \leq Pe_c$ we immediately obtain $\tilde{d} = 0$, $\tilde{u} = A$.

The strong dependence of the distance d on Pe is shown in Fig. 4, as well as the much weaker relationship to
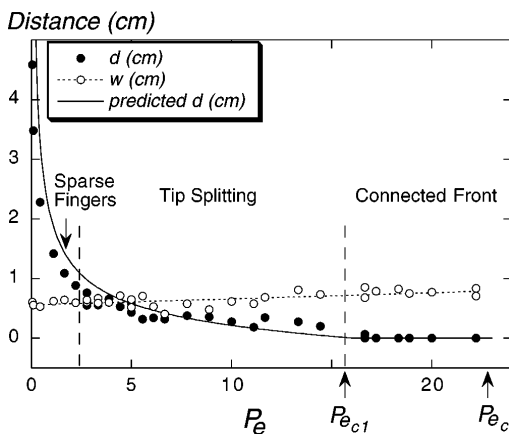
FIG. 4. The length scales d (full circles) and w (empty circles) as a function of Pe (at $h = 0.5$ cm). d is determined by the driving parameter, while w is weakly influenced by it. The slope of w(Pe) is 0.01 ± 0.002 cm (dashed line). The continuous line is a plot of the right-hand side of Eq. (3). It fits the measured d with no adjustable parameter.

the width w. The ratio between w and d characterizes the pattern and is determined by Pe. Sparse fingers are observed at $\frac{d}{w} \gg 1$ ($0.1 \leq$ Pe ≤ 2.6), tip splitting at $\frac{1}{4} \leq \frac{d}{w} \leq \frac{5}{4}$ ($2.6 <$ Pe $\leq$ Pe$_{c1}$). A connected front is observed at Pe$_{c1} \leq$ Pe $\leq$ Pe$_c$. In this regime $d = 0$ and w is the characteristic "cusp" size. Experimentally Pe$_c = 22 \pm 1$. w and d are not defined for Pe $\geq$ Pe$_c$. The agreement between data and theory [Eq. (3)], with no adjustable parameters, is very good. These measurements were performed by varying V_{O2} at $h = 0.5$ cm. Other values of h show the same behavior. It is possible that the slow linear increase of w as a function of V_{O2} is related to the limitation posed by the reaction rate.

There are a number of factors, related to heat transport, that contribute to the width of the finger w. Most dominant is the gap height h: w increases linearly as a function of h (as in viscous fronts [8]). The measured linear dependence is $w(h) = (1.78 \pm 0.4)h + (0.07 \pm 0.01)$ cm ($h = 0$ is outside the experimental range). Second, w decreases (linearly) with added nonreacting (N_2) gas to the feeding mixture while holding the amount of input oxygen fixed. Third, w increased when we created a badly heat conducting bottom (placing the sample on a thin foil above a cavity).

By carrying out the experiment in narrow pieces of paper ($L \approx d$) we could show that while d is collectively determined by the transport of reactants (through Pe), w is a feature of the individual finger and is not related to the size of the system [9]. Interestingly, tip splitting also occurs with an individual finger, if the fuel available to it (system size L) is larger than one finger but smaller than two ($w < L < 2w$). A full theory incorporating all relevant heat transport mechanisms would yield an effective Lewis number (ratio of thermal to mass diffusivities) and should predict both the instability onset Pe$_c$ and the finger width w.

The independence of global and local length scales is a general property of fingering instabilities. The global scale is determined by the overall supply of reactants and the local scale by processes that occur at the front. Looking beyond combustion, we have found evidence that the same growth rules apply to electrochemical deposition. In some regimes of this system the distance between branches is determined by the current density (supply of ions), analogous to the oxidizing wind in combustion [11]. The functional dependence of the distance between branches on the current density is then obtained using the same considerations as here, yielding a reasonably good description of the experimentally measured distances [9].

In conclusion, the complex burning process exhibits a rich but controllable pattern. We have shown that the fingering occurs in the absence of convection, and characterized the developed nonlinear state, in which fingers propagate at constant average velocity, width, and distance. Although heat transport plays a key role in the instability, our phenomenological model shows that the reactant transport alone determines the front velocity and the spacing between fingers. This simplified theory uses no free parameters, utilizes simple dynamic concepts, and works remarkably well. Future attention should focus on the onset regime, where preliminary observations already revealed interesting time-dependent modes.

[1] M. Faraday, *The Chemical History of a Candle,* edited by W. Crookes (Chato Windus, London, 1882).

[2] G. I. Sivashinsky, Annu. Rev. Fluid Mech. **15**, 179 (1983); Trans. R. Soc. London A **332**, 135 (1990).

[3] M. Gorman *et al.,* Phys. Rev. Lett. **76**, 228 (1996).

[4] T. Kashiwagi and S. L. Olson, in *Proceedings of SUMP-3* (National Academy of Science, Washington, DC, 1997).

[5] J. de-Ris, *Twelfth Symposium on Combustion* (Combustion Institute, Pittsburgh, 1969); J. Zhang *et al.,* Physica (Amsterdam) **189A**, 383 (1992).

[6] Y. Zhang *et al.,* Combust. Flame **90**, 71 (1992).

[7] A. P. Aldushin and B. J. Matkowsky, Combust. Sci. Technol. **133**, 293 (1998).

[8] P. Pelce, *Dynamics of Curved Fronts* (Academic Press, New York, 1988); J. Krug and H. Spohn, *Solids Far From Equilibrium* (Cambridge University, Cambridge, 1992).

[9] O. Zik, Ph.D. thesis, The Weizmann Institute of Science, 1998; O. Zik and E. Moses (to be published).

[10] To calculate this slope we used $a = 1$, $\rho_{O2} = 1.376 \times 10^{-3}$ g/cm^3, $\tau_{ub} = 0.018 \pm 0.002$ cm, $\mu = 1.18$ (cellulose), and $\rho_{ub} = 0.66 \pm 0.05$ g/cm^3. The values $\tau_b = 0.01 \pm 0.003$ cm and $\rho_b = 0.3 \pm 0.03$ g/cm^3 are the result of averaging over ten samples in the V_{O2} range of 0.5–15 cm/s. Both τ_b and ρ_b increase in that range but do not change by more than 20%.

[11] O. Zik and E. Moses, Phys. Rev. E **53**, 1760 (1996).